Title

Catecholaminergic A1/C1 neurons contribute to the maintenance of upper airway muscle tone but may not participate in NREM sleep-related depression of these muscles

Permalink

https://escholarship.org/uc/item/6ww6s333

Authors

Rukhadze, Irma
Carballo, Nancy J
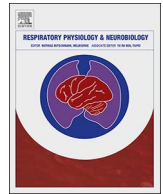Bandaru, Sathyajit S
et al.

Publication Date

2017-10-01

DOI

10.1016/j.resp.2017.07.001

Peer reviewed

CrossMark

Catecholaminergic A1/C1 neurons contribute to the maintenance of upper airway muscle tone but may not participate in NREM sleep-related depression of these muscles

Irma Rukhadze[a,b,c,d,*], Nancy J. Carballo[a], Sathyajit S. Bandaru[c], Atul Malhotra[f], Patrick M. Fuller[c,d], Victor B. Fenik[a,e]

[a] Department of Veterans Affairs, Greater Los Angeles Healthcare System, Los Angeles, CA, USA
[b] Department of Medicine, David Geffen School of Medicine at UCLA, Los Angeles, CA, USA
[c] Department of Neurology, Beth Israel Deaconess Medical Center, Boston, MA, USA
[d] Division of Sleep Medicine, Harvard Medical School, Boston, MA, USA
[e] WebSience International, Los Angeles, CA, USA
[f] Division of Pulmonary, Critical Care and Sleep Medicine, University of California San Diego, La Jolla, CA, USA

ARTICLE INFO

ABSTRACT

Neural mechanisms of obstructive sleep apnea, a common sleep-related breathing disorder, are incompletely understood. Hypoglossal motoneurons, which provide tonic and inspiratory activation of genioglossus (GG) muscle (a major upper airway dilator), receive catecholaminergic input from medullary A1/C1 neurons. We aimed to determine the contribution of A1/C1 neurons in control of GG muscle during sleep and wakefulness. To do so, we placed injections of a viral vector into DBH-cre mice to selectively express the hMD4i inhibitory chemoreceptors in A1/C1 neurons. Administration of the hM4Di ligand, clozapine-N-oxide (CNO), in these mice decreased GG muscle activity during NREM sleep ($F_{1,1,3}$ = 17.1, p < 0.05); a similar non-significant decrease was observed during wakefulness. CNO administration had no effect on neck muscle activity, respiratory parameters or state durations. In addition, CNO-induced inhibition of A1/C1 neurons did not alter the magnitude of the naturally occurring depression of GG activity during transitions from wakefulness to NREM sleep. These findings suggest that A1/C1 neurons have a net excitatory effect on GG activity that is most likely mediated by hypoglossal motoneurons. However, the activity of A1/C1 neurons does not appear to contribute to NREM sleep-related inhibition of GG muscle activity, suggesting that A1/C1 neurons regulate upper airway patency in a state-independent manner.

1. Introduction

Obstructive sleep apnea (OSA) is a sleep-related breathing disorder that has a prevalence of 13% in men and 6% of women in the United States (Peppard et al., 2013). OSA is characterized by recurrent episodes of partial or complete upper airway obstruction during sleep due to, at least in part, a depressant effect of sleep on upper airway muscle tone (Jordan et al., 2014). Individuals with chronic OSA are at increased risk for neurocognitive, cardiovascular, and metabolic disorders (Kheirandish et al., 2005; Pack and Gislason, 2009; Dempsey et al., 2010; Djonlagic et al., 2012; Veasey, 2012; Macey et al., 2013; Jordan et al., 2014; De Luca Canto et al., 2015). Despite substantial advances in both clinical and basic research, our understanding of the neural

mechanisms underlying OSA pathogenesis and the circuitry involved in atonia of upper airway muscles remains incomplete.

Among upper airway muscles that are innervated by hypoglossal motoneurons (XIImns) (Dobbins and Feldman, 1995; Altshuler et al., 1994; Saboisky et al., 2007; Fregosi and Ludlow, 2014), the genioglossus (GG) muscle is the most important dilator because its activation increases airway caliber (Remmers et al., 1978; Brennick et al., 2009). The activity of both XIImns and GG muscle is reduced during non-rapid eye movement (NREM) sleep and it is further suppressed during rapid eye movement (REM) sleep (Sauerland and Harper, 1976; Suratt et al., 1988; Horner et al., 1989; Richard and Harper, 1991; Mezzanotte et al., 1992; Katz and White, 2004; Saboisky et al., 2007; Eckert et al., 2009).

Neural mechanisms of depression of XIImns and GG muscle activity

during NREM and REM sleep have been extensively studied in different animal models, with the majority of these studies focused on mechanisms of XIImns depression during REM sleep. From these studies, two divergent mechanistic hypotheses have emerged: postsynaptic inhibition vs. disfacilitation, i.e. withdrawal of excitatory inputs. Glycinergic postsynaptic inhibition has been found to be responsible for the atonia of postural muscles during REM sleep and was suggested to play a role in REM-related depression of XIImn (Chase et al., 1989; Soja et al., 1991; Yamuy et al., 1999; Fung and Chase, 2015). In contrast, follow-on experiments indicated that GABA and glycine might not be involved in the depression of XIImns during REM sleep (Kubin et al., 1993; Morrison et al., 2003; Fenik et al., 2005a). The withdrawal of monoaminergic drive to XIImns during REM sleep remains, arguably, the most experimentally supported mechanism of REM sleep-related suppression of XIImns (Fenik et al., 2004, 2005a, 2005b; Chan et al., 2006). In addition, recent work has suggested that acetylcholine-mediated postsynaptic inhibition may contribute to sleep-related depression of XIImns in behaving rats (Grace et al., 2013).

With respect to monoaminergic mechanisms, serotonergic (5HT) and noradrenergic (NA) drive to XIImns originates from brainstem 5HT and NA neurons that have axonal projections to the XII nucleus (Aldes et al., 1992; Manaker and Tischler, 1993; Rukhadze and Kubin, 2007; Rukhadze and Fuller, 2015) and exhibit state-dependent patterns of activity (Aston-Jones and Bloom, 1981; Reiner, 1986; Jacobs and Azmitia, 1992; Rukhadze et al., 2008). As the contribution of NA to depression of XII nerve activity during REM sleep-like state was determined to be relatively stronger than 5HT in both, anesthetized (Fenik et al., 2005a; Fenik, 2015; Kubin, 2014, 2016) and behaving rats (Sood et al., 2005; Chan et al., 2006), our research activity has focused most intensively on NA mechanisms. The role of different pontine NA neurons was assessed in functional studies, which have concluded that among the NA groups tested (A5, A7, SubC and LC) A7 neurons provide the major NA excitatory drive to XIImns (Fenik et al., 2002, 2008, 2012). Importantly, however, the role of A1/C1 neurons was not tested in these previous studies. Therefore, we sought to determine the effect of acute inhibition of A1/C1 neurons on the activity of GG muscle in naturally sleeping mice using a chemogenetic approach.

In the present study, we tested the following two hypotheses: 1) A1/C1 CA neurons contribute to the maintenance of XIImns activity, and 2) the activity of A1/C1 neurons contributes to state-dependent modulation of XIImns. A preliminary report has been published (Rukhadze et al., 2014a,b, 2015).

2. Materials and methods

2.1. Animals

Adult male mice Tg(Dbh-cre)KH212Gsat/Mmucd or $B_6 \cdot$FVB(Cg)-Tg(Dbh-cre)KH212Gsat/Mmucd (henceforth DBH-cre; C57BL/6 background) originally obtained from the Mutant Mouse Regional Resource Center at the University of California, Davis, CA (stock # 032081 or 036778-UCD) (DePuy et al., 2013)) (8–12 weeks, 25–32 g, n = 19) were used in this study. Using stringent exclusionary criteria, data from only four mice had acceptable GG/Neck EMGs and EEG signal recordings, i.e., with no evidence of malfunction of GG implanted electrodes and successful placement of AAV injections into the A1/C1 region at approximately same AP level, were used for data analysis. Three mice were used in acute anesthetized experiments to optimize GG electrode implantation and two mice were used for anatomical analysis of Cre-dependent gene expression in CA neurons. The remaining ten mice were excluded on the basis of post-mortem histological analysis that revealed 1) recording sites within the tongue muscles that were not located near the base of the tongue, and/or 2) AAV injections that missed the target site.

In this line of DBH-cre mice, Cre recombinase was introduced upstream of the ATG start codon of the Dbh gene using the BAC clone RP23-354N13. This modification results in the expression of Cre recombinase that is under the control of the dopamine β-hydroxylase (DBH) promoter, hence Cre recombinase is expressed in all brainstem catecholaminergic (CA) neurons. DBH-cre mice were bred at our animal facility and underwent genotyping using the tail DNA PCR analysis. All procedures have been approved by the Institutional Animal Care and Use Committee of the Veterans Administration of Greater Los Angeles Healthcare system (VAGLAHS).

2.2. Mouse validation

Our initial goal was to identify a transgenic line of mice with little to no ectopic expression of the Cre-dependent gene beyond CA neurons. We therefore performed validation experiments on DBH-cre and TH-cre mice and compared Cre-dependent gene expression in CA neurons between the two mouse lines. To confirm that Cre activity mapped to brainstem regions of DBH-cre mice where the CA neurons are located as well as to assess the extent of ectopic expression, we used brain sections from the F1 progeny of adult, male DBH-cre mouse crossed with a tdTomato (*tandem dimer derivative of DsRed*) Cre-reporter (JAX B6;129S6-Gt(ROSA)26Sortm(CAG-tdTomato)Hze/J stock #007905/Ai9 or Ai9(RCL-tdT) (Madisen et al., 2010)). In these reporter mice, neurons that produce Cre-recombinase induce the expression of tdTomato (a red fluorescent protein variant). TH-cre mice B6.Cg-Tg(Th-cre)1Tmd/J were obtained from the Jackson laboratories (stock # 008601). The TH-cre mice have TH-cre transgene with a 9 Kb rat tyrosine hydroxylase (TH) promoter, directing expression of Cre recombinase to catecholaminergic cells. We used brain sections from the F1 progeny of adult, male TH-cre mouse crossed with a cre dependent GFP reporter mouse (*R26–loxSTOPlox–L10–GFP* strain). In these F1 mice, neurons that produce Cre-recombinase activates *RpL10* and yields eGFP-fused L10-ribosomal subunit expression (Krashes et al., 2014). Both reporter strains permit excellent visualization of whole neurons. Following, validation of the DBH-cre and TH-cre lines, and finding that DBH-cre mice has significantly less ectopic expression, we crossed heterozygote DBH-cre mice with C57/6J mice to generate heterozygote DBH Cre-driver mice that were used in our experiments (see Results). Given ATG targeting of Cre recombinase, we did not use homozygous DBH-cre mice in our experiments.

2.3. Surgery and stereotaxic injections of AAV vector into the A1/C1 of mice

Mice of at least 8 weeks of age were anesthetized with ketamine/xylazine intraperitoneally (IP, 100 and 10 mg/kg, respectively) and placed in a stereotaxic apparatus. Bilateral injections of an adeno-associated viral (AAV) vector expressing the hM4Di receptor in a Cre-dependent manner (hSyn-Dio-hM4Di-mCherry-AAV10; henceforth AAV-hM4Di; Fig. 1A) were placed into the medullary A1/C1 regions (Fig. 1B) (coordinates: 1.0 mm lateral from the midline, 1.1 mm caudal to the obex, and 1.0 mm deep from the medulla surface). Microinjections were made using a fine-tipped glass micropipette (tip diameter 15–20 μm) by an air pressure-driven delivery system. The injected volume (50 nL) was monitored during the injection by observing the fluid meniscus movement in the pipette through a calibrated microscope. The injection suspension contained AAV (3.4×10^{12} vector genome copies/ml) expressing a Cre-dependent hM4Di. Each injection was made slowly (3–5 min) and was followed by a delay of 3 min before the pipette was slowly retracted. Following the injections, muscles and skin overlying the 4th ventricle were separately sutured and animals were observed until full recovery. Mice were then returned to their original cages for at least 4–5 weeks that are necessary for the full expression of hM4Di receptors (Anaclet et al., 2014, 2015; Venner et al., 2016).
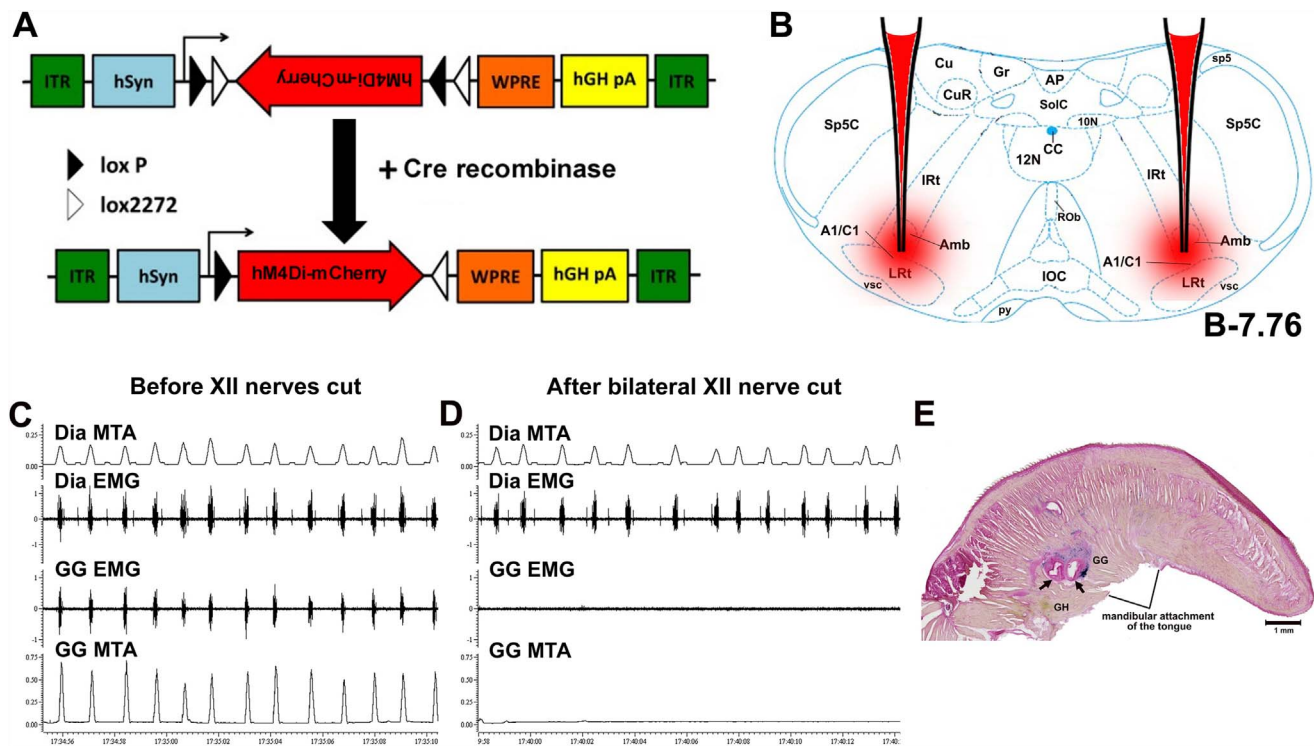
Fig. 1. Details of injected hSyn-DIO-hM4Di-mCherry (hM4Di-mCherry) vector and the effect of sectioning of both XII nerves on GG EMG in anesthetized mouse. (A) The vector employs the FLEX switch strategy to achieve cre-mediated transgene inversion between LoxP recombination sites and expression of a functional hM4Di-mCherry product in neurons expressing cre-recombinase. (B) Coronal medullary section from a mouse brain atlas (Paxinos and Franklin, 2008) showing the injection target (CA neurons in A1/C1 region) in a DBH-Cre mouse. (C) An example of tongue and diaphragm EMGs recorded in a mouse with intact XII nerves. (D) The continuation of the recording in the same mouse after bilateral sectioning of XII nerves that abolished the tongue EMG whereas diaphragm EMG was preserved. (E) Example of two GG muscle recording sites in the tongue (arrows) demonstrated by iontophoretic deposition of iron ions revealed as blue marks by the Prussian blue reaction. Abbreviations: ITR, inverted terminal repeat; WPRE, woodchuck hepatitis posttranscriptional regulatory element; hSyn, the human synapsin 1 promoter; Sp5C, spinal trigeminal nucleus, caudal; sp5, spinal trigeminal tract; Cu, cuneate nucleus; CuR, cuneate nucleus, rotundus part; Gr, gracile nucleus; AP, area postrema; SolC, bucleus solitary tract, commissural; 10N, dorsal motor nucleus, vagus; CC, central canal; 12N, hypoglossal nucleus; IRt, intermediate reticular nucleus; Amb, ambiguus nucleus; Rob, raphe obscurus nucleus; LRt, lateral reticular nucleus; IOC, inferior olive, subnucleus C of mediate nucleus; py, pyramidal tract; vsc, ventral spinocerebellar tract; A1, noradrenaline/C1, adrenaline cells. MTA, moving time average; GH, geniohyoid muscle; GG, genioglossus muscle.

2.4. Positioning of GG and Dia EMGs electrodes for acute and chronic experiments

To establish landmarks to position GG EMG electrodes within the mouse tongue we recorded GG and diaphragmatic (Dia) EMGs in mice (n = 3) under ketamine/xylazine anesthesia (100/10 mg/kg, IP). For GG and Dia muscle recordings two Teflon-insulated stainless steel multi-stranded wires (A-M systems, 0.003/0.0055" bare/coated diameter) were used. A midline incision was made inferior to the jaw and the skin overlying the digastric muscle (a jaw opener) was retracted laterally to expose the pharyngeal region of the mouse. The recording ends of the wires had insulation removed over ~0.3 mm and were inserted into a 26 gauge injection needle (Monoject, Hypodermic needle 26GA ½; 0.45 mm x 12.7 mm) slightly bent to form the circle shape. The anterior belly of digastricus was separated into two parts at the midline and for each wire the needle was inserted into the ventral surface of the tongue on the opposite sides of the midline, toward the base of the tongue close to the mandibular symphysis. Implantation of GG electrode closer to this point at the mandible produces less instability of the muscle-electrode interface thereby reducing scarring, which improves signal quality (I. Rukhadze, unpublished observations in rats and mice). Each time when the needle was gently withdrawn leaving the wire in the tongue, the wire was tied to the tongue surface by two knots using non-absorbable silk sutures. To record activity of the diaphragm, the same wires with insulation removed over ~10 mm at the recording end were passed through the sternal diaphragm on both sides of the midline and the bared ends of the wires were anchored to the inferior part of the sternum. GG and Dia recording electrodes were connected to the recording amplifiers and, if needed, the depth of the

GG recording electrodes was optimized by gentle repositioning of the inserted wires until a strongly modulated inspiratory EMG could be recorded (Morrison et al., 2002; Polotsky et al., 2011) concomitant to the diaphragmatic activity (Fig. 1, panel C, as an example). In separate experiments, sectioning of XII nerves on both sides abolished the activity that was recorded with GG recording electrodes, which confirmed that the recorded inspiratory EMG was fully controlled by XII motoneurons (Fig. 1C, D). The respiratory modulation of the tongue EMG in addition to the location of recording electrodes inclined that the activity was originating from GG muscle. Subsequent histology verified the locations of EMG electrode tips within boundaries of the GG muscle (Fig. 1E).

2.5. Instrumentation for monitoring of sleep-wake behavior and genioglossus muscle activity

Two weeks after AAV injections, mice were anesthetized with ketamine/xylazine IP (100 and 10 mg/kg, respectively) and implanted with two EEG screw electrodes (Pinnacle Technology) and a pair of neck electromyogram (EMG) flexible electrodes with sockets (Plastics One) that were previously soldered to a 6-pin connector (Heilind Electronics Inc.). For the recording of GG muscle activity, EMG electrodes were implanted bilaterally into the tongue at its pharyngeal region as described above. The free wire ends were tunneled subcutaneously towards to the head and connected to the miniature 6-pin connector (together with the neck wires and those attached to the EEG screws). The assembly was secured to the skull with dental cement (A-M Systems). The scalp wound was closed with surgical sutures and the mouse was given antibiotic (Metacam, 5 mg/kg, i.m.) and analgesic

(Buprenprphine, 0.5 mg/kg, i.m.). Following surgery, the mice were kept in a warm environment until normal body activity was resumed and they were returned to home cages.

2.6. HM4Di-AAV and CNO

hSyn-DIO-hM4Di-mCherry AAV, serotype 10 (Anaclet et al., 2014, 2015; Venner et al., 2016) was used in our experiments. This mutated channel does not respond to endogenous acetylcholine but is selectively activated by a synthetic and pharmacologically inert ligand, CNO, which produces cell hyperpolarization through the Gi pathway. This gene has been cloned in reverse orientation (so-called double inverted orientation), so that a nonsense transcript is produced until the transgene is exposed to cre-recombinase, which flips the gene into the sense orientation. The cassette confers great selectivity, without transcriptional 'leakage' in cells that lack Cre. The DREADD was also fused to mCherry so that receptor expression can be visualized and monitored. The channel construct was subsequently packaged into an AAV vector (hSyn-DIO-hM4Di-mCherry-AAV10). The particular version of inhibitory DREADD used in this study was previously developed and rigorously validated both in vitro and in vivo and is described in detail in the following references (Anaclet et al., 2014, 2015; Venner et al., 2016).

2.7. Habituation and recording procedures

Four weeks after AAV-hM4Di injections, each mouse was connected to a recording cable and habituated to recording conditions for 2–4 h in a plethysmograph (Buxco Electronics) that was located inside an insulated soundproof recording chamber illuminated with a 12 V DC LED lights. The plethysmograph was ventilated with continuous flow of air (0.2–0.4 L/min at 22–24 °C) and allowed measuring respiratory rate and tidal volume. During the habituation days, optimal gains for all signals were established to obtain maximal amplification without saturation of the amplifiers or converters at times of maximal activity and were kept constant during all subsequent recording sessions. EEG, neck EMG and GG EMG were recorded in a bipolar configuration and amplified with the following bandwidths: 0.3–100 Hz for EEG and 30–1000 Hz for both EMG signals (Model 78 B amplifiers, Grass, Warwick, RI, USA). All signals were continuously monitored and digitally stored using sampling rates of $300 \, s^{-1}$ for EEG and $2000 \, s^{-1}$ for EMGs (Power–1401 A/D converter and Spike–2 v.7 data acquisition system; Cambridge Electronic Design, Inc., Cambridge, England). During recording sessions, all signals (EEG, neck and GG muscle activity, and animal's respiration parameters that were derived from the plethysmograph) were recorded for 7 h (from 10:00 to 17:00) as following. After 2 h of baseline period (10:00–12:00), saline (control) or CNO (0.3 mg/kg, Sigma-Aldrich; (Anaclet et al., 2014, 2015; Venner et al., 2016)) were injected IP at 12:00 PM The injection effects were monitored during 5 h following the injections (12:00–17:00). In order to minimize the possibility of GG electrode failure, often caused by scarring from surgical implantation or misplacement of the tip of recording electrodes, we conducted our experiments on subsequent days rather than in a randomized sequence. Therefore, all animals received control injections of saline on the first experimental day and CNO injections on the next day (in 24 h after saline injection).

2.8. Scoring of sleep-wake states and data analysis

Data analysis was performed on animals that have satisfactory recordings of EEG and neck/GG EMGs, i.e., the recorded signals correlated with the state transitions and followed the behavioral activity of the animal with no evidence of malfunction of the implanted electrodes and with verified location of recording electrodes in the GG muscle. The behavioral states were defined using 1) the Spike-2 scoring and spectral analysis script by 10-s epochs according to the state that occupied more

than 50% of the epoch duration; 2) visual analysis of the cortical and neck signals, and 3) the Spike-2 power spectrum analysis of cortical EEG. Wakefulness was recognized based on the presence of a low-amplitude and high frequency "desynchronized" EEG accompanied with a high amplitude erratic neck EMG. NREM was characterized by a high-amplitude and low frequency "synchronized" EEG accompanied by a low level and relatively stable neck EMG and a regular respiratory rate. REM sleep followed relatively prolonged periods of NREM sleep and was defined based on the desynchronized EEG with a prominent peak in the power spectrum at 5–8 Hz ("theta rhythm"), further reduction of neck EMG ("muscle atonia") followed by muscle twitches that increase toward the end of REM sleep, and an irregular respiratory rate. We calculated the duration of wakefulness, NREM and REM sleep; the tidal volume and respiratory rate; and the mean amplitude of rectified neck and GG EMG. The measurements were obtained during 1 h periods "before" saline/CNO injections (from 11:00 to 12:00) and "after" saline/CNO injections (from 15:00 to 16:00).

2.9. Statistical analysis

For statistical analyses of the CNO effect, we used two-tailed paired Student's *t*-test and two way repeated measures analysis of variance (ANOVA) with two factors: saline vs. CNO and before vs. after injections. The variability of means is characterized by the standard error (SE) throughout the report. Differences were considered significant at $p < 0.05$.

2.10. Histological procedures

Mice were deeply anesthetized with ketamine (100 mg/kg) and transcardially perfused with 100 mL of phosphate-buffered saline (PBS) at room temperature followed by 50 mL of 10% Formalin in PBS. Brains were removed, post-fixed overnight in formalin-PBS at 4 °C and, after cryoprotection in 20% sucrose-PBS, were cut into 40 μm-thick coronal sections on a cryostat. Separate 1-in-3 series of brain tissue sections were collected.

2.11. Immunofluorescence

To verify the expression of hM4Di receptor in A1/C1 neurons, we double-labeled sections from experimental DBH-cre mice with a rabbit polyclonal antibody that binds dsRed-derived red-fluorescent proteins to enhance the native fluorescence of mCherry and visualize hM4Di expression, and anti-TH sheep polyclonal antibody, a marker for CA neurons. Sections were washed in PBS, and incubated in primary dsRed antisera (1:10,000, cat. #632496, Clontech) and TH (1:2000, cat. #AB1542, Millipore) diluted in PBS containing 0.25% Triton X-100 (PBST), for 12–24 h at 20–24 °C. Sections were then washed in PBS and incubated in secondary antiserum Cy3-tagged anti-rabbit IgG (for dsRed; 1:500; Jackson ImmunoResearch Laboratories); and Alexafluor488-tagged donkey anti-sheep antibody (for TH; 1:500; Invitrogen) diluted in PBST for 2 h. Sections were then washed in PBS, mounted on Superfrost Plus slides, dried overnight, cover-slipped using Prolong Gold antifade mountant (Molecular probes #P36930), and stored in slide folders at 4 °C until imaging. In all animals, we verified AAV-hM4Di injection sites in the A1/C1 region using the fluorescent and confocal microscopes (Zeiss LSM 710).

2.12. Histological verification of GG muscle recording sites in the tongue

Prior to perfusion, in deeply anesthetized mice, a low intensity (18 μA) positive current was passed through the GG recording electrodes for 60 s to deposit iron ions (Fig. 1E). After the perfusion, tongues were removed, postfixed and cryoprotected and serially cut into 50 μm parasagittal sections and mounted. Using the Prussian blue iron staining kit (Polysciences, Inc #24199) that results in dark blue staining
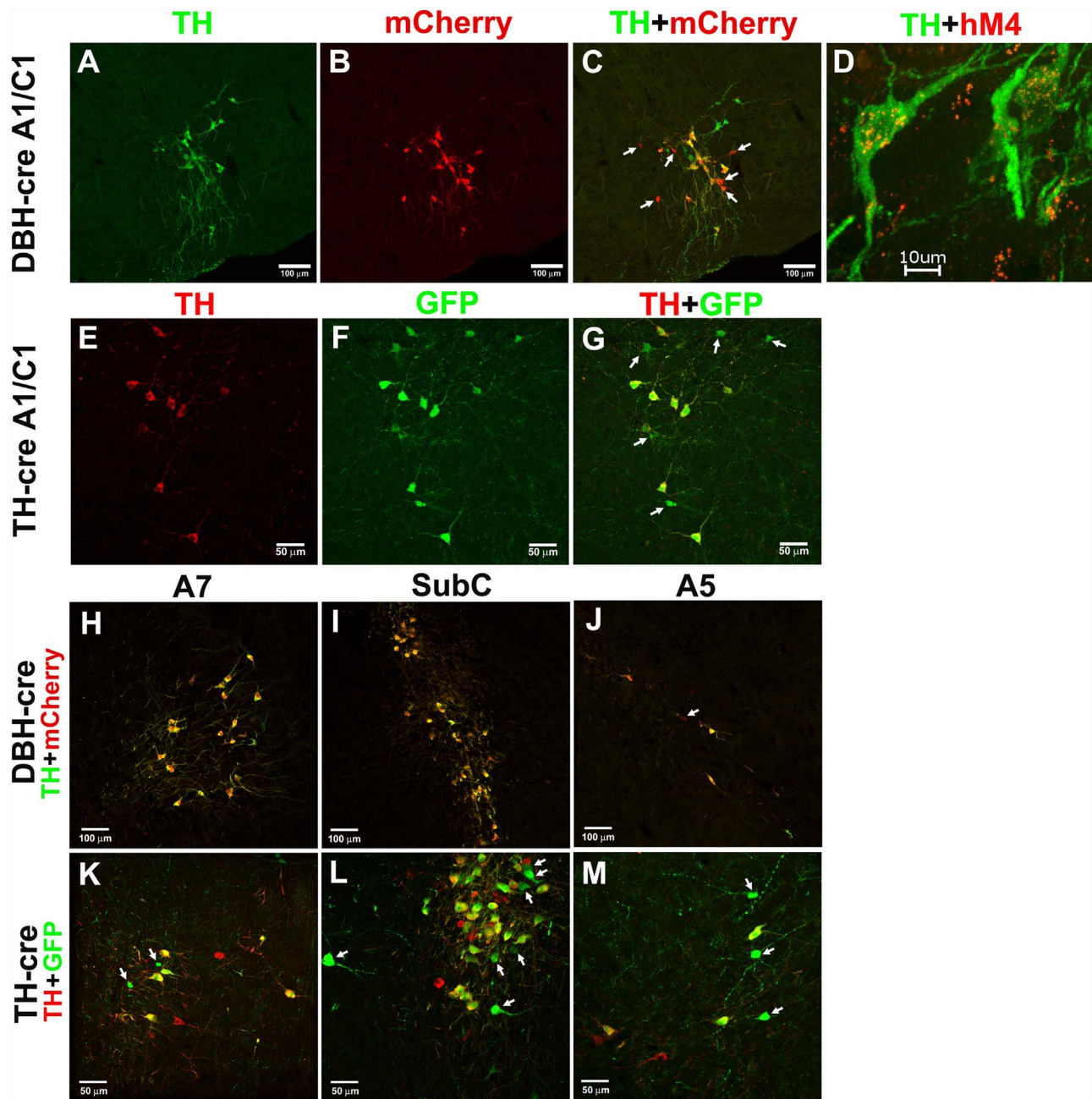
Fig. 2. Validation of DBH-cre and TH-cre mice and Cre-dependent expression of the hM4Di receptor in A1/C1 neurons of DBH-cre mice. Brainstem sections from a DBH-cre, lox-TdTomato mouse that were processed for (A) TH (green neurons) and (B) mCherry (red neurons) immunofluorescence to evaluate (C) the Cre-mediated expression of tdTomato protein in TH-positive A1/C1 neurons. (D) A confocal image of A1/C1 neurons showing double-labeling for mCherry and TH from a mouse injected with AAV-hM4Di into the A1/C1 region indicating DREADD expression (red fluorescence) in the TH-positive (green fluorescence) A1/C1 neurons. Brainstem sections from a TH-cre, GFP mouse that were processed for (E) TH (red neurons) and (F) GFP (green neurons) immunofluorescence to evaluate (G) the Cre-mediated expression of GFP protein in TH-positive A1/C1 neurons. Merged photomicrographs show that in A7, SubC and A5 region in DBH-cre mice (H, I J), immunostaining for TH (green) colocalizes with mCherry (red) and in TH-cre mice (K, L, M) immunostaining for TH (red) colocalizes with GFP (green). Arrows point to Cre-dependent gene expression in non-TH A1C1 and A5 neurons in DBH-cre (C, J) and TH-cre mice (G, M) and in A7 and SubC neurons in TH-cre mice (K, L). (For interpretation of the references to colour in this figure legend, the reader is referred to the web version of this article.)

of iron deposit (Fig. 1E), we verified the location of GG recording electrodes with a brightfield microscope at 4x and 10x (Olympus CHBS).

3. Results

3.1. Cre-dependent gene expression in brainstem catecholaminergic neurons of DBH- and TH-cre mice

We compared specificity of Cre-dependent gene expression in brainstem SubC, A7, A5 and A1/C1 CA neurons between transgenic TH-cre mice and the more recently developed DBH-cre mice. In the TH-cre mice Cre recombinase is under the control of tyrosine hydroxylase (TH) promoter whereas in DBH-cre mice Cre-recombinase is expressed under the DBH promoter in all CA cells. Following dual fluorescent immunohistochemistry, we examined the distribution pattern of TH-positive (TH+) (Fig. 2A, green), tdTomato-positive (tdTomato+) (Fig. 2B, red) and double-labeled (Fig. 2C, yellow-orange color) A1/C1 neurons in a DBH-cre mouse. We found that the distributions of TH+ CA neurons in locus coeruleus (LC), sub-coeruleus (SubC), A7, A5 and A1/C1 in both mouse lines are similar to that described previously in rats (Rukhadze and Kubin, 2007; Rukhadze et al., 2008). We counted

the total number of TH+ neurons, double labeled TH+/tdTomato+ and TH-/tdTomato+ (ectopic expression) in these CA regions. The ectopic expression (number of TH-/tdTomato+ neurons relative to the total tdTomato+ neurons) in DBH-cre mice mouse (n = 1) was lower for most CA regions (SubC 0.0%, A7 0.0%, A5 25.0%, A1/C1 30.0%) (Fig. 2C, H, I, J) as compared to TH-cre mouse (n = 1) (SubC 18.9%, A7 22.2%, A5 50.0%, A1/C1 35.7%) (Fig. 2G, K, L, M). Ectopic expression of a cre-dependent gene detected in these mouse lines might be related to transient promoter activity during development, as has been demonstrated in several other cre lines (Vong et al., 2011; Venner et al., 2016). In addition, eutopic expression (number of TH+/tdTomato+ neurons relative to the total TH+ neurons) in SubC, A7, A5 and A1/C1 regions tended to be higher in DBH-cre mice when compared to the TH-cre mice (84.2% ± 7.9 *vs.* 79.6% ± 9.0). We therefore opted to use DBH-cre mice rather than TH-cre mice for our study. As expected, injections of AAV-hM4Di into the A1/C1 of this line of DBH-cre mice show strong co-expression of the hM4Di receptor expression (red) in TH + A1/C1 neurons (green) (Fig. 2D).

3.2. Recording of genioglossus muscle activity in naturally sleeping mice

All experimental mice following habituation to the plethysmograph chamber and recording conditions (Fig. 3A) exhibited normal pattern of the sleep-wake behavior. During wakefulness, the GG and neck muscles displayed the highest amplitude of tonic or phasic activity (Fig. 3B). The amplitude of both GG and neck muscle activity was significantly reduced and became more stable and predominantly tonic during NREM sleep. The REM sleep atonia in the GG muscle always preceded that in neck muscles, which occurred at the transition from NREM to REM sleep. The characteristic phasic "twitches" in GG muscle activity appeared during REM sleep and gradually increased toward the end of this state. Despite a strong inspiratory modulation under anesthesia, the GG muscle activity had mostly non-respiratory pattern of activity and only occasionally, inspiratory activity occurring during NREM sleep. Overall, the behavior of GG muscle activity was similar to that in rats (Rukhadze et al., 2011, 2014a,b; Grace et al., 2013).

3.3. Inhibition of A1/C1 CA neurons specifically decreases GG muscle activity in freely behaving mice

When measured during NREM sleep, selective inhibition of A1/C1 neurons by CNO injections into the DBH-cre mice expressing hM4Di receptors in A1/C1 neurons resulted in suppression of tonic GG muscle activity as compared with saline (control) injections in the same mice (n = 4) (Fig. 4A). Mean GG muscle activity during NREM sleep tended to increase from the morning measurements (before saline injections) and the measurements made afternoon (after saline injections) in control experimental sessions: from 31.6 AU (arbitrary units) + 12–37.2 AU + 13. However, CNO injections reduced mean GG muscle activity from 34.9 AU + 7.8 to 28.1 AU + 5.4 (Fig. 4B). The depressant effect of CNO on GG EMG was statistically significant ($F_{1,1,3}$ = 17.1, p = 0.026, ANOVA, n = 4). In contrast with that observation, neither the amplitude of neck EMG, respiratory rate, tidal volume or the duration of states was changed during NREM sleep after the CNO when compared with saline injections in the same mice (Fig. 4C–F). These data suggest that chemogenetic inhibition of A1/C1 neurons has a specific effect on GG muscle activity.

The relative changes in GG and neck EMG after the saline/CNO injections were compared to their EMG levels before the injections during NREM sleep (Fig. 5). In control sessions, the relative increase of GG muscle activity after saline injection was to 122% + 6.0. The CNO injection decreased GG EMG to 81.8% + 4.6 relative to its pre-injection level (p < 0.01, paired *t*-test, n = 4). The relative changes for neck EMG were essentially the same in both control and CNO sessions: 97.7% + 2.4 and 94.7% + 5.7, respectively. The individual effects of CNO on GG muscle activity were consistent in the magnitude and direction in all animals (Fig. 5B).

During wakefulness, CNO injections tended to decrease the amplitude of GG EMG (180 AU + 39 before and 120 AU + 37 after, CNO) as compared to saline sessions (153 AU + 24 before and 142 AU + 37 after, saline). In relative units GG EMG decrease also tended to be larger in CNO sessions as compared to saline sessions: 72.7% + 20 vs. 91.2% + 18 (not significant, paired *t*-test, n = 4). During REM sleep, the CNO injections had no effect on GG EMG because the activity of GG muscle showed no activity during REM sleep and hence an effect of CNO could
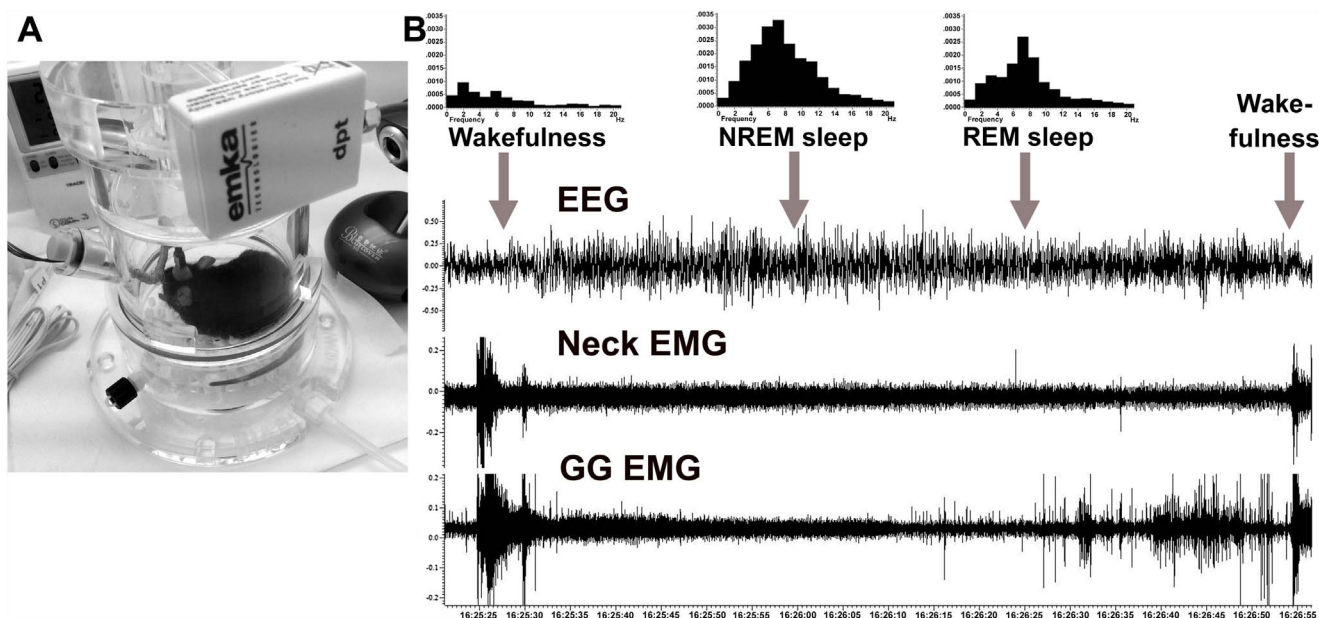

Fig. 3. A representative recording of GG muscle activity during wakefulness, NREM- and REM-sleep in a behaving DBH-cre mouse. (A) An experimental mouse placed in a plethysmograph chamber, which is ventilated with room air for recordings of GG muscle activity and behavioral states. (B) An example of state-dependent activity of GG muscle in a naturally sleeping mouse. GG muscle activity is markedly decreased during transition from wakefulness to NREM sleep and further reduced during transition from NREM to REM sleep. During REM sleep, the GG muscle generates intense twitches with gradually increasing intensity towards the end of the state. The histograms show characteristic power spectra of EEG during wakefulness, NREM and REM sleep.
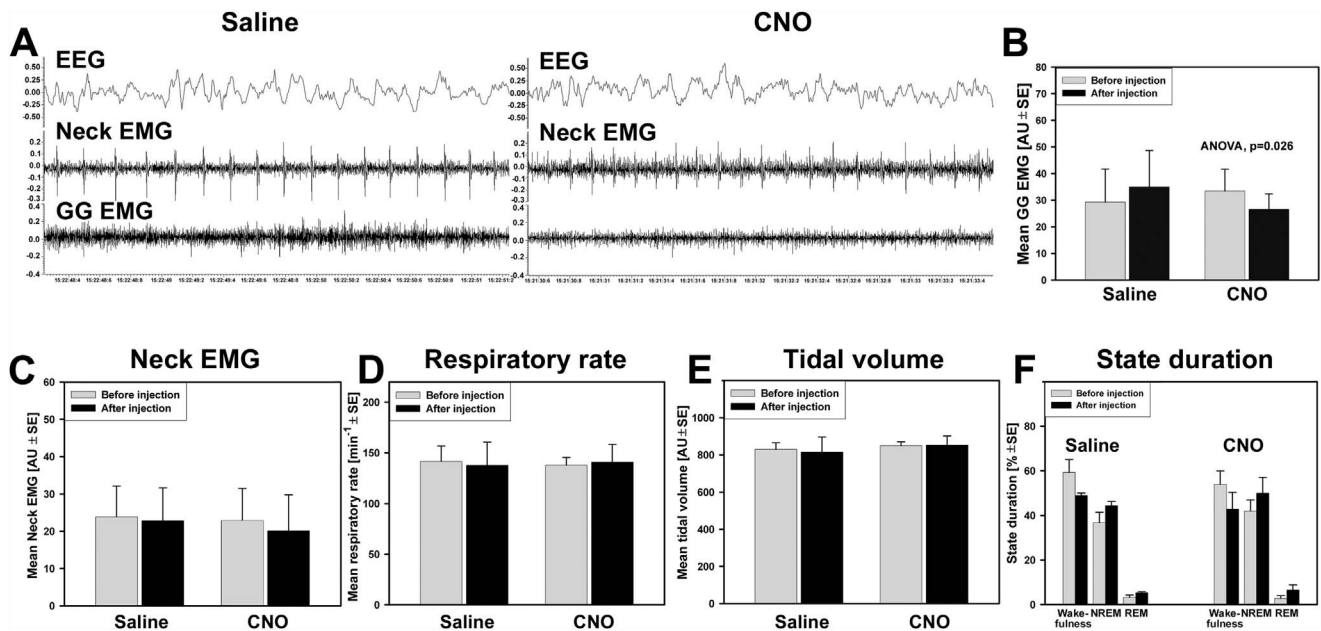
Fig. 4. The effect of CNO-induced inhibition of A1/C1 CA neurons on GG muscle activity in DBH-cre mouse expressing hM4Di receptor in A1/C1 neurons during NREM sleep. (A) GG muscle activity recorded during NREM sleep after control injection of saline (left panel). The GG muscle activity, which was recorded during NREM sleep at the same circadian time on the next day, was markedly decreased after CNO (0.3 mg/kg) injection during in the same animal (right panel). (B) Mean data of the amplitude of GG EMG shows a tendency for an increase of GG muscle activity following saline injections likely due to circadian changes in the GG muscle activity in these animals. However, during next day CNO sessions, the amplitude of GG EMG significantly decreased after CNO injections ($F_{1,1,3} = 17.1$, $p = 0.026$, two way repeated measures ANOVA). The acute inhibition of A1/C1 CA neurons did not affect amplitude of neck muscle EMG (C), respiratory rate (D), tidal volume (E) or the state durations (F).
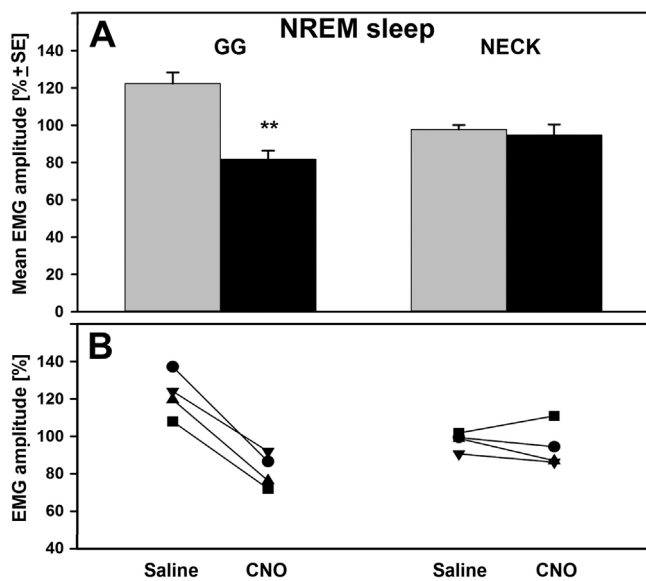

Fig. 5. Effect of saline and CNO on GG and neck muscle activity calculated relative to pre-injection levels. (A) The bars show the mean changes in the amplitude of EMG that was measured after saline/CNO injections and expressed relative to that before the injections during NREM sleep. During saline sessions, the relative GG muscle activity increased to 122% + 6.0 whereas during CNO sessions that activity decreased to 81.8% + 4.6 of pre-injection control ($p < 0.01$, t-test). The relative amplitude of neck EMG was not affected by CNO. (B) Individual responses of GG and neck muscle activity to saline ad CNO in each animal.

not be determined.

3.4. Effect of CNO on the magnitude of sleep-related depression of GG muscle activity

Our next objective was to determine whether acute inhibition of A1/C1 neurons altered the magnitude of relative suppression of GG muscle activity that occurs following transitions from wakefulness to
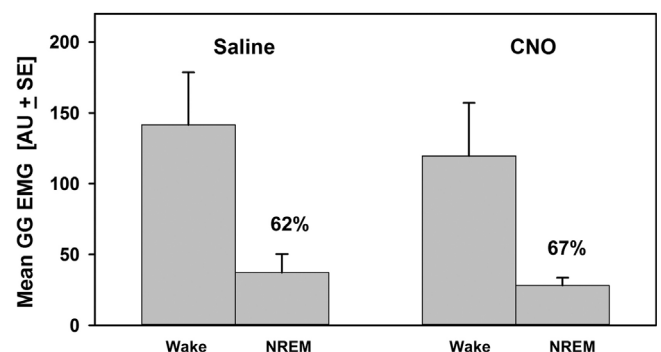

Fig. 6. Effect of CNO on depression of GG muscle activity that occurs during transition from wakefulness to NREM sleep. The bars show post-injection measurements of the GG EMG amplitude during wakefulness and NREM sleep. After saline, the GG EMG reduced significantly from wakefulness to NREM sleep (the relative NREM-induced GG depression was 62%). After CNO injections, the amplitude of GG muscle activity during both wakefulness and NREM sleep tended to decrease as compared to saline sessions, however, the relative NREM-induced GG muscle depression was 67% (the difference was not statistically significant). If the activity of A1/C1 neurons contributed to the NREM-induced GG muscle depression, then the relative magnitude of the NREM-related GG muscle depression would be decreased after CNO injections as compared to saline. The absence of changes in this depression, or even a tendency to increase (from 62% to 67%), suggests that A1/C1 neurons do not contribute to the NREM-related GG muscle depression.

NREM sleep. After saline injections, the GG muscle activity decreased during NREM sleep by 62.1% + 21 (n = 4) relative to its activity during wakefulness (Fig. 6). The mean GG muscle activity decreased during both wakefulness and NREM sleep after CNO injections (Fig. 6). However, and contrary to our expectations, NREM-induced depression of GG muscle activity following CNO injections was 66.6% + 11, which was similar or higher to that obtained after saline injections.

4. Discussion

This is the first study to report on the activity of the GG muscle in behaving mice and to assess the functional role of CA A1/C1 neurons in

the control of GG muscle activity during sleep and wakefulness. The major findings of this study are 1) the activity of A1/C1 neurons has a net excitatory effect on GG muscle activity; and 2) the activity of A1/C1 CA neurons does not contribute to NREM sleep-related suppression of GG muscle activity.

Important advances in understanding the neural mechanisms of sleep-related depression of upper airway motoneurons have been made over the past three decades with multiple neurotransmitter systems now implicated in REM sleep-related depression of XIImns. Yet the neuronal circuitry underlying the upper airway muscle depression during NREM sleep and REM sleep has not been fully identified and characterized. The research conducted to date has been largely focused on the mechanisms mediating REM sleep-related depression of XIImns, as XIImns innervate the muscles of the upper airway (Zauerland and Harper, 1976; Remmers, 1978; Mezzanotte et al., 1992; Fenik et al., 2004, 2005b; Saboisky et al., 2007; Kubin, 2014, 2016). Two major competing theories have argued that REM sleep-related depression of activity in upper airway muscles results from either postsynaptic inhibition (increased glycine and/or GABA hyperpolarization) or disfacilitation (decreased serotonergic and noradrenergic excitation) of XIImns.

The first direct evidence that glycine is an essential neurotransmitter for mediating REM sleep-related atonia of postural muscles was provided in studies using behaving cats (Soja et al., 1991). General support for postsynaptic inhibition of XIImns during REM sleep derives from a microdialysis study showing that levels of GABA and glycine are increased in the hypoglossal nucleus during REM sleep (Kodama et al., 2003). However, other studies testing the direct role of GABA and/or glycine antagonists in REM sleep-related depression of XIImns in different animal models such as decerebrated cats (Kubin et al., 1993), anesthetized rats (Fenik et al., 2005b), and freely behaving rats (Morrison et al., 2003) have reported little or no effect of glycine/GABA$_A$ receptor antagonists on the suppression of XIImns or GG muscle activity during either REM sleep or REM sleep-like state. Hence consensus on this important mechanistic issue remains lacking.

The hypothesis that withdrawal of monoaminergic drive to XIImns during REM sleep might underlie changes in GG activity has received support from direct pharmacological studies (Fenik et al., 2004, 2005a, 2005b; Chan et al., 2006). For example, depression of XII nerve activity during carbachol-elicited REM sleep-like state can be pharmacologically abolished by microinjections of combination of GABA, glycine, NA and 5HT antagonists into XIImns in urethane anesthetized rats (Fenik et al., 2004). It has also been shown that a combination of NA and 5HT antagonists is both necessary and sufficient to abolish depression of XII nerve activity during REM sleep-like state (Fenik et al., 2005a), with the contribution of NA being larger than 5HT (Fenik et al., 2005a; Kubin, 2014, 2016; Fenik, 2015). These findings were confirmed by reports that NA has a significant contribution to REM sleep-related depression of GG muscle activity in naturally sleeping behaving rats (Chan et al., 2006) whereas the contribution of 5HT was minimal (Sood et al., 2005).

The role of glutamate and acetylcholine in REM sleep-related depression of XIImns has been suggested by an *in-vitro* study, in which glutamatergic excitation of XIImns was presynaptically inhibited by muscarinic mechanisms (Bellingham and Berger, 1996). However, the investigation of glutamatergic mechanisms in behaving rats did not provide sufficient evidence to either support or refute the role of glutamate in this phenomenon (Steenland et al., 2008). In addition, no changes in the level of glutamate were detected in XII motor nucleus during REM sleep (Kodama et al., 2003). Recently, muscarinic inhibition has been reported to play a significant role in REM sleep-related depression of GG muscle activity mediated by G-protein-coupled inwardly rectifying potassium channels in behaving rats (Grace et al., 2013).

The density of NA terminals that closely apposed to GG motoneurons in the ventral region of XII nucleus increased in rats that were exposed to chronic-intermittent hypoxia, i.e., conditions mimicking OSA (Rukhadze et al., 2010). This finding is consistent with increased GG muscle tone in OSA patients (Mezzanotte et al., 1992). In our previous anatomical studies using retrograde tracers, we showed that the A1/C1, A7, LC, SubC and A5 neurons provide innervation of the XIImns (Rukhadze and Kubin, 2007). The individual contribution of each of these NA cell populations to the innervation of the XII nucleus was highest for A5 neurons and lowest for LC neurons (ibid). Recently, using conditional anatomic tracers in TH-cre mice, we examined the projections from A1/C1 neurons to XIImns and found TH-positive anterogradely labeled axon terminals within the ventral sub-division of the XII nucleus that innervates the GG muscle (Rukhadze and Fuller, 2015).

Brainstem NA neurons of the LC (Aston-Jones and Bloom, 1981) and SubC (Reiner, 1986) reduce their activity during NREM sleep and are virtually silent during REM sleep. In addition, Fos expression in A2/C2, A5, SubC and A7 neurons strongly correlates with parameters of pharmacologically induced REM sleep-like states, which suggests a state-dependent nature of their activity, whereas A1/C1 neurons did not show a significant correlation (Rukhadze et al., 2008). The fact that A1/C1 neurons did not significantly decrease their activity during REM sleep-like states could be explained by activation of C1 neurons during REM sleep-like state (Stettner et al., 2013). Clearly, further studies are needed to dissociate the mixed population of A1/C1 neurons and establish the functional relationship between GG muscle activity and noradrenergic A1 and adrenergic C1 neurons during sleep-wake states in behaving mice.

NA mechanisms appear to make an important contribution to REM sleep-induced depression of XIImns and the role of NA neurons in maintenance of XIImns activity was assessed in previous functional studies. For example, it was found that clonidine-induced decrease in activity of A7 neurons, but not A5, LC or SubC neurons, reduced activity of XIImns in anesthetized rats (Fenik et al., 2002, 2008, 2012). As indicated, the role of A1/C1 neurons was not tested in these studies. We therefore decided to investigate the effect of inhibition of A1/C1 neurons on upper airway muscles in behaving animals using the DREADD technique because 1) precise targeting of neural structures by nanoliter microinjections of agonists and antagonists is not feasible in behaving animals, and 2) the microdialysis approach can potentially damage the A1/C1 nucleus in mice. In addition, by using the DREADD technique we were afforded the opportunity to work with behaving animals and thereby assess the contribution of A1/C1 neurons to state-dependent modulation of GG muscle activity. We found that AAV-hM4Di receptor-mediated inhibition of A1/C1 neurons specifically decreased the activity of GG muscle during NREM sleep and had a tendency to do so during wakefulness.

Since A1/C1 neurons do not demonstrate strong state-dependent activity (Rukhadze et al., 2008), the contribution of these neurons to state-dependent modulation of XIImns activity would not have necessarily been predicted. However, as stated, it is possible that presynaptic mechanisms (Bellingham and Berger, 1996) might control the release of NA from the A1/C1 terminals to XIImns and, if so, this would permit A1/C1 neurons to contribute to state-dependent depression of GG muscle. We tested this hypothesis by analyzing the relative decrease of GG muscle activity during the transition from wakefulness to NREM sleep. If our hypothesis were correct, one would expect that the relative NREM sleep-induced depression of GG muscle activity would decrease after CNO as compared to saline injections. However, NREM-induced GG muscle depression did not decrease further following CNO injections, suggesting that the activity of A1/C1 does not contribute to the naturally occurring inhibition of GG muscle during transitions from wakefulness to NREM sleep. We did not test the effect of CNO on GG muscle inhibition during REM sleep for reasons that are discussed below.

In this study, our assessment focused on A1/C1 inhibition of GG muscle activity under normal isocapnic condition. Under this condition, similarly to naturally sleeping rats (Rukhadze et al., 2011, 2014a,

2014b; Fenik et al., 2013), GG muscle activity was absent during REM sleep in our mice precluding the quantification of CNO effects during this state. We did not use CO_2 to activate GG activity over the concern that doing so would potentially affect experimental outcomes. However, stimulation of breathing with physiological levels of CO_2 would be less of a concern if one were to study the relative contribution of different modulators of GG muscle activity under the same hypercapnic conditions during REM sleep state.

A1/C1 neurons may activate XIImns directly or indirectly or both. Our preliminary findings suggest that A1/C1 neurons may directly innervate XIImns (Rukhadze and Fuller, 2015). However, A1/C1 neurons project extensively in the brain (Tucker et al., 1987; Card et al., 2006; Abbott et al., 2013) and therefore indirect pathways may also contribute to the activation of XIImns by A1/C1. This suggestion, however, is not supported by our data that show an absence of CNO-induced changes in neck EMG, respiratory parameters (respiratory rate and tidal volume) or in the duration of vigilance states (wakefulness, NREM sleep and REM sleep).

As CA neurons in A1/C1 region are implicated in cardiovascular control (Abbott et al., 2009; Guyenet et al., 2013; Burke et al., 2014), CNO could affect blood pressure, but this was not assessed in our experiments. However, we believe that any possible influence of blood pressure changes, secondary to CNO administration, on GG activity was negligible for two reasons: 1) since A1 neurons provide inhibitory control over C1 neurons (Granata et al., 1985), the simultaneous inhibition of both neural groups by CNO in our experiments likely resulted in minor or no changes in blood pressure; 2) since an increase in blood pressure inhibits respiratory discharges but not tonic activity in hypoglossal nerve (Wasicko et al., 1993), changes in blood pressure were unlikely to affect the tonic GG activity that was recorded in our experiments. In addition, we cannot exclude the possibility that inactivation of A1/C1 neurons during wakefulness may have reduced the frequency of oral behaviors (i.e., eating, drinking, grooming etc.), which, in turn, could have contributed to the tendency of GG activity to decrease.

Recent data provide support for the concept that the mechanisms underlying OSA may vary across individuals, with some patients exhibiting anatomical predisposition, others showing dysfunction in upper airway dilator muscles, and yet others having unstable ventilatory control or some combination of abnormalities (Veasey, 2012; Eckert et al., 2013). OSA patients experience upper airway obstruction only during sleep, whereas during wakefulness they maintain upper airway patency and adequate ventilation (Remmers, 1978; Mezzanotte et al., 1992). Decreased activity of XIImns that innervate upper airway dilator muscles during sleep may thus play a key role in a subset of OSA patients (Jordan et al., 2014). In fact, for these patients electrical stimulation of hypoglossal nerve effectively decreases the apnea/hypopnea index (Strollo et al., 2014; Schwartz et al., 2014; Kezirian et al., 2014). Studies of single motor units in humans have also revealed considerable complexity of upper airway motor control (Saboisky et al., 2007; Nicholas et al., 2010; Trinder et al., 2014). More human studies in combination with more basic studies such as the present one will be required to define new therapeutic approaches for OSA.

In summary, our data demonstrate that medullary A1/C1 CA neurons, similar to previously established pontine A7 noradrenergic neurons, are involved in control of upper airway muscle activity (Fenik et al., 2008). We found that acute and selective inhibition of A1/C1 neurons 1) decreased the activity of the GG muscle during NREM sleep, but 2) does not alter the magnitude of naturally occurring depression of GG muscle during transitions from wakefulness to NREM sleep. These findings suggest that A1/C1 neurons represent an important state-independent mechanism to protect upper airway from collapse during sleep onset in OSA patients.

Disclosures

Acknowledgments

References

Abbott, S.B., Stornetta, R.L., Socolovsky, C.S., West, G.H., Guyenet, P.G., 2009. Photostimulation of channelrhodopsin-2 expressing ventrolateral medullary neurons increases sympathetic nerve activity and blood pressure in rats. J. Physiol. 587, 5613–5631.

Abbott, S.B., Depuy, S.D., Nguyen, T., Coates, M.B., Stornetta, R.L., Guyenet, P.G., 2013. Selective optogenetic activation of rostral ventrolateral medullary catecholaminergic neurons produces cardiorespiratory stimulation in conscious mice. J. Neurosci. 33, 3164–3177.

Aldes, L., Chapman, M., Chronister, R., Haycock, J., 1992. Sources of noradrenergic afferents to the hypoglossal nucleus in the rat. Brain Res. Bull. 29, 931–942.

Altshuler, S.M., Bao, X., Miselis, R.R., 1994. Dendritic architecture of hypoglossal motoneurons projecting to extrinsic tongue musculature in the rat. J. Comp. Neurol. 342, 538–550.

Anaclet, C., Ferrari, L., Arrigoni, E., Bass, C.E., Saper, C.B., Lu, J., Fuller, P.M., 2014. GABAergic parafacial zone is a medullary slow-wave-sleep promoting center. Nat. Neurosci. 9, 1217–1224.

Anaclet, C., Pedersen, N.P., Ferrari, L.L., Venner, A., Bass, C.E., Arrigoni, E., Fuller, P.M., 2015. Basal forebrain control of wakefulness and cortical rhythms. Nat. Commun. 6, 8744.

Aston-Jones, G., Bloom, F.E., 1981. Activity of norepinephrine-containing locus coeruleus neurons in behaving rats anticipates fluctuations in the sleep-waking cycle. J. Neurosci. 1, 876–886.

Bellingham, M.C., Berger, A.J., 1996. Presynaptic depression of excitatorysynaptic unputs to rat hypoglossal motoneurons by muscarinic M2 receptors. J. Neurophysiol. 76, 3758–3770.

Brennick, M.J., Pack, A.I., Ko, K., Kim, E., Pickup, S., Maislin, G., Schwab, R.J., 2009. Altered upper airway and soft tissue structures in the New Zealand obese mouse. Am. J. Respir. Crit. Care Med. 179, 158–169.

Burke, P.G., Abbott, S.B., Coates, M.B., Viar, K.E., Stornetta, R.L., Guyenet, P.G., 2014. Optogenetic stimulation of adrenergic C1 neurons causes sleep state-dependent cardiorespiratory stimulation and arousal with sighs in rats. Am. J. Respir. Crit. Care Med. 190, 1301–1310.

Card, J.P., Sved, J.C., Craig, B., Raizada, M., Vazquez, J., Sved, A.F., 2006. Efferent projections of rat rostroventrolateral medulla C1 catecholamine neurons: implications for the central control of cardiovascular regulation. J. Comp. Neurol. 499, 840–859.

Chan, E., Steenland, H., Liu, H., Horner, R., 2006. Endogenous excitatory drive modulating respiratory muscle activity across sleep-wake states. Am. J. Respir. Crit. Care Med. 174, 1264–1273.

Chase, M., Soja, P., Morales, F., 1989. Evidence that glycine mediates the postsynaptic potentials that inhibit lumbar motoneurons during the atonia of active sleep. J. Neurosci. 9, 743–751.

De Luca Canto, G., Pachêco-Pereira, C., Aydinoz, S., Major, P.W., Flores-Mir, C., Gozal, D., 2015. Biomarkers associated with obstructive sleep apnea and morbidities: a scoping review. Sleep Med. 16, 347–357.

DePuy, S.D., Stornetta, R.L., Bochorishvili, G., Deisseroth, K., Witten, I., Coates, M., Guyenet, P.G., 2013. Glutamatergic neurotransmission between the C1 neurons and the parasympathetic preganglionic neurons of the dorsal motor nucleus of the vagus. J. Neurosci. 33, 1486–1497.

Dempsey, J.A., Veasey, S.C., Morgan, B.J., O'Donnell, C.P., 2010. Pathophysiology of sleep apnea. Physiol. Rev. 90, 47–112.

Djonlagic, I., Saboisky, J., Carusona, A., Stickgold, R., Malhotra, A., 2012. Increased sleep fragmentation leads to impaired offline consolidation of motor memories in humans. PLoS One 7, e34106.

Dobbins, E.G., Feldman, J.L., 1995. Differential innervation of protruder and retractor muscles of the tongue in rat. J. Comp. Neurol. 357, 376–394.

Eckert, D.J., Malhotra, A., Lo, Y.L., White, D.P., Jordan, A.S., 2009. The influence of obstructive sleep apnea and gender on genioglossus activity during rapid eye movement sleep. Chest 135, 957–964.

Eckert, D.J., White, D.P., Jordan, A.S., Malhotra, A., Wellman, A., 2013. Defining phenotypic causes of obstructive sleep apnea. Identification of novel therapeutic targets. Am. J. Respir. Crit. Care Med. 188, 996–1004.

Fenik, V., Marchenko, V., Janssen, P., Davies, R.O., Kubin, L., 2002. A5 cells are silenced when REM sleep-like signs are elicited by pontine carbachol. J. Appl. Physiol. 93, 1448–1456.

Fenik, V., Davies, R., Kubin, L., 2004. Combined antagonism of aminergic excitatory and amino acid inhibitory receptors in the XII nucleus abolishes REM sleep-like depression of hypoglossal motoneuronal activity. Arch. Ital. Biol. 142, 237–249.

Fenik, V., Davies, R., Kubin, L., 2005a. REM sleep-like atonia of hypoglossal (XII) motoneurons is caused by loss of noradrenergic and serotonergic inputs. Am. J. Respir. Crit. Care Med. 172, 1322–1330.

Fenik, V., Davies, R., Kubin, L., 2005b. Noradrenergic, serotonergic and GABAergic antagonists injected together into the XII nucleus abolish the REM sleep-like depression of hypoglossal motoneuronal activity. J. Sleep Res. 14, 419–429.

Fenik, V.B., Rukhadze, I., Kubin, L., 2008. Inhibition of pontine noradrenergic A7 cells reduces hypoglossal nerve activity in rats. Neurosci 157, 473–482.

Fenik, V.B., Marchenko, V., Davies, R.O., Kubin, L., 2012. Inhibition of A5 neurons facilitates the occurrence of REM sleep-like episodes in urethane-anesthetized rats: a new role for noradrenergic A5 neurons? Front. Neurol. 3, 119.

Fenik, V.B., Fung, S.J., Lim, V., Chase, M.H., 2013. Quantitative analysis of the excitability of hypoglossal motoneurons during natural sleep in rats. J. Neurosci. Meth. 212, 56–563.

Fenik, V.B., 2015. Revisiting antagonist effects in hypoglossal nucleus: brainstem circuit for the state-dependent control of hypoglossal motoneurons: a hypothesis. Front. Neurol. 6, 254.

Fregosi, R.F., Ludlow, C.L., 2014. Activation of upper airway muscles during breathing and swallowing. J. Appl. Physiol. 116, 291–301.

Fung, S.J., Chase, M.H., 2015. Postsynaptic inhibition of hypoglossal motoneurons produces atonia of the genioglossus muscle during rapid eye movement sleep. Sleep 38, 139–146.

Grace, K.P., Hughes, S.W., Horner, R.L., 2013. Identification of the mechanism mediating genioglossus reactivation muscle suppression in REM sleep. Am. J. Respir. Crit. Care Med. 187, 311–319.

Granata, A.R., Kumada, M., Reis, D.J., 1985. Sympathoinhibition by A1-noradrenergic neurons is mediated by neurons in the C1 area of the rostral medulla. J. Auton. Nerv. Syst. 14, 387–395.

Guyenet, P.G., Stornetta, R.L., Bochorishvili, G., Depuy, S.D., Burke, P.G., Abbott, S.B., 2013. Invited review EB 2012: C1 neurons: the body's EMTs. Am. J. Physiol. Regul. Integr. Comp. Physiol. 305, R187–R204.

Horner, R.L., Shea, S., McIvor, J., Guz, A., 1989. Pharyngeal size and shape during wakefulness and sleep in patients with obstructive sleep apnoea. Q. J. Med. 72, 719–735.

Jacobs, B.L., Azmitia, E.C., 1992. Structure and Function of the brain serotonin system. Physiol. Rev. 72, 165–229.

Jordan, A.S., McSharry, D.G., Malhotra, A., 2014. Adult obstructive sleep apnoea. Lancet 383, 736–747.

Katz, E.S., White, D.P., 2004. Genioglossus activity during sleep in normal control subjects and children with obstructive sleep apnea. Am. J. Respir. Crit. Care Med. 170, 553–560.

Kezirian, E.J., Goding Jr., G.S., Malhotra, A., O'Donoghue, F.J., Zammit, G., Wheatley, J.R., Catcheside, P.G., Smith, P.L., Schwartz, A.R., Walsh, J.H., Maddison, K.J., Claman, D.M., Huntley, T., Park, S.Y., Campbell, M.C., Palme, C.E., Iber, C., Eastwood, P.R., Hillman, D.R., Barnes, M., 2014. Hypoglossal nerve stimulation improves obstructive sleep apnea:12-month results. J. Sleep Res. 23, 77–83.

Kheirandish, L., Gozal, D., Pequignot, J.M., Pequignot, J., Row, B.W., 2005. Intermittent hypoxia during development induces long-term alterations in spatial working memory, monoamines, and dendritic branching in rat frontal cortex. Pediatr. Res. 58, 594–599.

Kodama, T., Lai, Y.Y., Siegel, J.M., 2003. Changes in inhibitory amino acid release linked to pontine- induced atonia: an in vivo microdialysis study. J. Neurosci. 23, 1548–1554.

Krashes, M.J., Shah, B.P., Madara, J.C., Olson, D.P., Strochlic, D.E., Garfield, A.S., Vong, L., Pei, H., Watabe-Uchida, M., Uchida, N., Liberles, S.D., Lowell, B.B., 2014. An excitatory paraventricular nucleus to AgRP neuron circuit that drives hunger. Nature 507, 238–242.

Kubin, L., Kimura, H., Tojima, H., Davies, R., Pack, A., 1993. Suppression of hypoglossal motoneurons during the carbachol-induced atonia of REM sleep is not caused by fast synaptic inhibition. Brain Res. 611, 300–312.

Kubin, L., 2014. Sleep-wake control of the upper airway by noradrenergic neurons, with and without hypoxia. Prog. Brain Res. 209, 255–274.

Kubin, L., 2016. Neural control of the upper airway: respiratory and state-dependent mechanisms. Comp. Physiol. 6, 1801–1850.

Macey, P.M., Kumar, R., Woo, M.A., Yan-Go, F.L., Harper, R.M., 2013. Heart rate responses to autonomic challenges in obstructive sleep apnea. PLoS One 8, e76631.

Madisen, L., Zwingman, T.A., Sunkin, S.M., Oh, S.W., Hatim, A., Zariwala, H.A., Gu, H., Lydia, L., Ng, L.L., Palmiter, R.D., Hawrylycz, M.J., Jones, A.R., Lein, E.S., Zeng, H., 2010. A robust and high-throughput Cre reporting and characterization system for the whole mouse brain. Nat. Neurosci. 13, 133–140.

Manaker, S., Tischler, L.J., 1993. Origin of serotonergic afferents to the hypoglossal nucleus in the rat. J. Comp. Neurol. 334, 466–476.

Mezzanotte, W.S., Tangel, D.J., White, D.P., 1992. Waking genioglossal electromyogram in sleep apnea patients versus normal controls (a neuromuscular compensatory mechanism). J. Clin. Invest. 89, 1571–1579.

Morrison, J.L., Sood, S., Liu, X., Liu, H., Park, E., Nolan, P., Horner, R.L., 2002. Glycine at hypoglossal motor nucleus: genioglossus activity, CO(2) responses, and the additive effects of GABA. J. Appl. Physiol. 93, 1786–1796.

Morrison, J.L., Sood, S., Liu, H., Park, E., Liu, X., Nolan, P., Horner, R.L., 2003. Role of inhibitory amino acids in control of hypoglossal motor outflow to genioglossus muscle in naturally sleeping rats. J. Physiol. 552, 975–991.

Nicholas, C.L., Bei, B., Worsnop, C., Malhotra, A., Jordan, A.S., Saboisky, J.P., Chan, J.K., Duckworth, E., White, D.P., Trinder, J., 2010. Motor unit recruitment in human genioglossus muscle in response to hypercapnia. Sleep 33, 1529–1538.

Pack, A.I., Gislason, T., 2009. Obstructive sleep apnea and cardiovascular disease: a perspective and future directions. Prog. Cardiovasc. Dis. 51, 434–451.

Paxinos, G., Franklin, K.B.J., 2008. The Mouse Brain in Stereotaxic Coordinates. Academic Press.

Peppard, P.E., Young, T., Barnet, J.H., Palta, M., Hagen, E.W., Hla, K.M., 2013. Increased prevalence of sleep-disordered breathing in adults. Am. J. Epidemiol. 177, 1006–1014.

Polotsky, M., Elsayed-Ahmed, A.S., Pichard, L., Richardson, R.A., Smith, P.L., Schneider, H., Kirkness, J.P., Polotsky, V., Schwartz, A.R., 2011. Effect of age and weight on upper airway function in a mouse model. J. Appl. Physiol. 111, 696–703.

Reiner, P.B., 1986. Correlational analysis of central noradrenergic neuronal activity and sympathetic tone in behaving cats. Brain Res. 378, 86–96.

Remmers, J.E., DeGroot, W.J., Sauerland, E.K., Anch, A.M., 1978. Pathogenesis of upper airway occlusion during sleep. J. Appl. Physiol. 44, 931–938.

Richard, C.A., Harper, R.M., 1991. Respiratory-related activity in hypoglossal neurons across sleep-waking states in cats. Brain Res. 542, 167–170.

Rukhadze, I., Fuller, P.M., 2015. Medullary A1 /C1 catecholaminergic neurons directly innervate hypoglossal motoneurons. Sleep 38 (Suppl), A47.

Rukhadze, I., Kubin, L., 2007. Differential pontomedullary catecholaminergic projections to hypoglossal motor nucleus and viscerosensory nucleus of the solitary tract. J. Chem. Neuroanat. 33, 23–33.

Rukhadze, I., Fenik, V., Branconi, J., Kubin, L., 2008. Fos expression in pontomedullary catecholaminergic cells following rapid eye movement sleep-like episodes elicited by pontine carbachol in urethane-anesthetized rats. Neurosci 152, 208–222.

Rukhadze, I., Fenik, V.B., Benincasa, K.E., Price, A., Kubin, L., 2010. Chronic intermittent hypoxia alters density of aminergic terminals and receptors in the hypoglossal motor nucleus. Am. J. Respir. Crit. Care Med. 182, 1321–1329.

Rukhadze, I., Kamani, H., Kubin, L., 2011. Quantitative differences among EMG activities of muscles innervated by subpopulations of hypoglossal and upper spinal motoneurons during non-REM sleep-REM sleep transitions: a window on neural processes in the sleeping brain. Arch. Ital. Biol. 149, 499–515.

Rukhadze, I., Kalter, J., Stettner, G.M., Kubin, L., 2014a. Lingual muscle activity across sleep-wake states in rats with surgically altered upper airway. Front. Neurol. 5, 61.

Rukhadze, I., Fuller, P.M., Fenik, V.B., 2014b. Acute inhibition of catecholaminergic A1/C1 neurons reduces genioglossus muscle activity in behaving mice. Soc. Nurosci (Abstr. A548.03).

Rukhadze, I., Fuller, P.M., Fenik, V.B., 2015. Do A1 /C1 catecholaminergic neurons contribute to sleep-related inhibition of genioglossus muscle activity? Sleep 38 (Suppl), A46.

Saboisky, J.P., Butler, J.E., McKenzie, D.K., Gorman, R.B., Trinder, J.A., White, D.P., Gandevia, S.C., 2007. Neural drive to human genioglossus in obstructive sleep apnoea. J. Physiol. 585, 135–146.

Sauerland, E.K., Harper, R.M., 1976. The human tongue during sleep: electromyographic activity of the genioglossus muscle. Exp. Neurol. 51, 160–170.

Schwartz, A.R., Smith, P.L., Oliven, A., 2014. Electrical stimulation of the hypoglossal nerve: a potential therapy. J. Appl. Physiol. 116, 337–344.

Soja, P., López-Rodríguez, F., Morales, F., Chase, M., 1991. The postsynaptic inhibitory control of lumbar motoneurons during the atonia of active sleep: effect of strychnine on motoneuron properties. J. Neurosci. 11, 2804–2811.

Sood, S., Morrison, J.L., Liu, H., Horner, R.L., 2005. Role of endogenous serotonin in modulating genioglossus muscle activity in awake and sleeping rats. Am. J. Respir. Crit. Care Med. 172, 1338–1347.

Steenland, H.W., Liu, H., Horner, R.L., 2008. Endogenous glutamatergic control of rhythmically active mammalian respiratory motoneurons in vivo. J. Neurosci. 28, 6826–6835.

Stettner, G.M., Lei, Y., Benincasa, H.K., Kubin, L., 2013. Evidence that adrenergic ventrolateral medullary cells are activated whereas precerebellar lateral reticular nucleus neurons are suppressed during REM sleep. PLoS One 8, e62410.

Strollo Jr., P.J., Soose, R.J., Maurer, J.T., de Vries, N., Cornelius, J., Froymovich, O., Hanson, R.D., Padhya, T.A., Steward, D.L., Gillespie, M.B., Woodson, B.T., Van de Heyning, P.H., Goetting, M.G., Vanderveken, O.M., Feldman, N., Knaack, L., Strohl, K.P., 2014. STAR Trial Group: upper-airway stimulation for obstructive sleep apnea. N. Engl. J. Med. 370, 139–149.

Suratt, P.M., McTier, R.F., Wilhoit, S.C., 1988. Upper airway muscle activation is augmented in patients with obstructive sleep apnea compared with that in normal subjects. Am. Rev. Respir. Dis. 137, 889–894.

Trinder, J., Jordan, A.S., Nicholas, C.L., 2014. Discharge properties of upper airway motor units during wakefulness and sleep. Prog. Brain Res. 212, 59–75.

Tucker, D.C., Saper, C.B., Ruggiero, D.A., Reis, D.J., 1987. Organization of central adrenergic pathways: I. Relationships of ventrolateral medullary projections to the hypothalamus and spinal cord. J. Comp. Neurol. 259, 591–603.

Veasey, S.C., 2012. Piecing together phenotypes of brain injury and dysfunction in obstructive sleep apnea. Front. Neurol. 3, 139.

Venner, A., Anaclet, C., Broadhurst, R.Y., Saper, C.B., Fuller, P.M., 2016. A novel population of wake-promoting GABAergic neurons in the ventral lateral hypothalamus. Curr. Biol. 26, 2137–2143.

Vong, L., Ye, C., Yang, Z., Choi, B., Chua Jr., S., Lowell, B.B., 2011. Leptin action on GABAergic neurons prevents obesity and reduces inhibitory tone to POMC neurons. Neuron 71, 142–154.

Wasicko, M.J., Giering, R.W., Knuth, S.L., Leiter, J.C., 1993. Hypoglossal and phrenic nerve responses to carotid baroreceptor stimulation. J. Appl. Physiol. 75, 1395–1403.

Yamuy, J., Fung, S., Xi, M., Morales, F., Chase, M., 1999. Hypoglossal motoneurons are postsynaptically inhibited during carbachol-induced rapid eye movement sleep. Neurosci 94, 11–15.